Stability Analysis and Control Technology of Gob-Side Entry Retaining with Double Roadways by Filling with High-Water Material in Gently inclined Coal Seam

Shengrong Xie
China University of Mining and Technology - Beijing Campus
En Wang
China University of Mining and Technology - Beijing Campus
Dongdong Chen (chendongbcg@163.com)
China University of Mining and Technology - Beijing Campus
Hui Li
China University of Mining and Technology - Beijing Campus
Zaisheng Jiang
China University of Mining and Technology - Beijing Campus
Hongzeng Yang
Hebei Coal Science Research Institute

Research

Keywords: High-water material, Gob-side entry retaining with double roadways, Stability analysis, Gently inclined coal seam, Control technology

Posted Date: June 29th, 2021

DOI: https://doi.org/10.21203/rs.3.rs-659048/v1

Stability analysis and control technology of gob-side entry retaining with double roadways by filling with high-water material in gently inclined coal seam

Shengrong Xie[a,b], En Wang[a], Dongdong Chen[a,*], Hui Li[a], Zaisheng Jiang[a], Hongzeng Yang[c]

[a] *School of Energy and Mining Engineering, China University of Mining & Technology-Beijing, Beijing 100083, China*

[b] *Beijing Key Laboratory for Precise Mining of Intergrown Energy and Resources, China University of Mining & Technology-Beijing, Beijing 100083, China*

[c] *Hebei Coal Science Research Institute Corporation Ltd., Xingtai 054000, China*

Abstract Roadside filling body in traditional gob-side entry retaining (GER) has several shortcomings such as the insufficient support resistance, the inability to adapt to the deformation of surrounding rock and isolate the goaf effectively. Taking the GER with double roadways by filling with 1.8-m-wide high-water material in gently inclined coal seam of Zuozegou mine as a project case, the mechanical model of GER with double roadways in the gently inclined coal seam is constructed, and the reasonable width of the filling body of GER is verified by combining with the peak strength of high-water material. The FLAC^{3D} numerical simulation method is used to study the distribution characteristics of stress and plastic zone of GER after being affected by the mining disturbance, and the failure range of surrounding rock of GER with double roadways is obtained. Based on this, a coupling control technology named anchor cables and bolts in the roof and solid coal + single props in entry-in support and goaf side of the outer roadway + anchor bolts in roadside high-water material + short anchor cables below the filling body is proposed and conducted in industrial test. Through the coupling methods of arranging borehole peeping and observing the convergences of surrounding rock, the stability of GER with double roadways is analyzed. The results show that GER with double roadways by filling with 1.8-m-wide high-water material has good control effect. The above research has played an active role in promoting the application of high-water material in roadside filling of GER.

Keywords: High-water material, Gob-side entry retaining with double roadways, Stability analysis, Gently inclined coal seam, Control technology

1. Introduction

Gob-side entry retaining (GER) with no-pillars has many advantages such as improving coal recovery rate, realizing Y-shaped ventilation, easing the mining and excavation replacement, saving excavation cost and has been widely used in all kinds of coal mines in China (Bai et al. 2015; Feng and Zhang 2015; He et al. 2017; Kong et al. 2021). The traditional roadside supports of GER have mainly experienced low-strength support methods such as wooden stacks, gangue belts, dense pillars and concrete blocks (Bai et al. 2004; Huang 2011; Yang et al. 2016). However, due to the shortcomings of traditional roadside supports such as resistance and shrinkage cannot adapt to the large deformation of surrounding rock, supports cannot effectively isolate the goaf and difficult to achieve high mechanization, it has been gradually eliminated. The new high-water material has several characteristics (Li and Liu 2018; Wu et al. 2020; Zhou et al. 2020) such as obvious plastic characteristic, quick solidification, fast increase of the resistance, high strength, a certain compression rate after curing, low cost and well adapt to the large deformation of surrounding rock of GER. In recent years, it has been gradually applied in roadside filling of GER in China. Therefore, it is of great significance to study the engineering application of high-water material in roadside filling of GER for mining safely, improving coal recovery rate and increasing economic benefits.

In the traditional roadside supports of GER, dense pillars are rarely used due to the problems of large supporting workload, poor supporting and isolation effects of the goaf (Zhang et al. 2020). The gangue stacking method (He et al. 2017) is easy to cause excessive roof sinking and result in poor stability, so the adaptability is small, and it is hard to

*Corresponding author at: School of Energy and Mining Engineering, China University of Mining & Technology-Beijing, Beijing 100083, China
E-mail address: chendongbcg@163.com (Dongdong Chen)

promote and apply. The prefabricated block masonry wall (Kang et al. 2010) can basically form a high-strength wall for isolating the goaf, but it still cannot solve the problem of the connection between the wall and the roof. It cannot be reliably sealed and its effect is bad. The concrete wall (Tang et al. 2010) has wide adaptability, high-bearing capacity, safety and reliability. However, the filling cost is high, and the construction is complicated and the strength increase speed cannot meet the needs of high-yield and high-efficiency of the working face, and there is a problem of slurry leakage. Although the concrete paste filling technology (Huang et al. 2015) can be obtained on the spot and environmentally friendly mining, it is difficult to be widely promoted due to the construction process and the paste strength. Therefore, the above-mentioned roadside supports have the disadvantages of supporting resistance and shrinkage cannot adapt to the large deformation of surrounding rock of GER, cannot effectively isolate the goaf and difficult to achieve high mechanization. In view of this, it is necessary to study new filling materials with suitable strength, shrinkage pressure and timely closure of the goaf.

The new high-water material has the characteristics of early strength, quick solidification, small volume strain, incompressibility under the action of three-dimensional force and obvious plastic characteristic, which is a new type of roadside filling material of GER. Compared with the traditional gob-side entry retaining, the 2202 GER in Zuozegou mine has following features: ①Occurrence conditions of gently inclined coal seam; ②Roadside filling body is 1.8-m-wide high-water material; ③Gob-side entry retaining with double roadway; ④The gangue in the goaf behind the working face is easy to enter the outer roadway of GER, as shown in Fig. 1. In view of the above characteristics of high-water material, as well as the majority of existing research results of GER are concentrated on the single retained roadway in the nearly horizontal coal seam, the background of this project is to fill the GER with double roadways by filling with high-water material in gently inclined coal seam in Zuozegou mine, China. The basic mechanical properties of high-water material are analyzed through laboratory tests. Based on the construction of mechanical model of GER with double roadways by filling with high-water material in gently inclined coal seam, the reasonable width of roadside high-water material of GER is determined. The FLAC^{3D} numerical simulation method is used to study the distribution characteristics of vertical stress and plastic zone of surrounding rock when the headgate is not disturbed and affected stably by the mining of 2202 working face. The failure range of surrounding rock of GER is revealed. A coupling control technology named anchor cables and bolts in the roof and solid coal + single props in entry-in support and goaf side of the outer roadway + anchor bolts in roadside high-water material + short anchor cables below the filling body is proposed and conducted in industrial test. Through the methods of arranging borehole peeping, observing the convergences of surrounding rock and measuring the load in the filling body, the control effects of surrounding rock of GER is systematically analyzed. The research results can play an active role in promoting the application of high-water material in roadside filling of GER in coal mines.

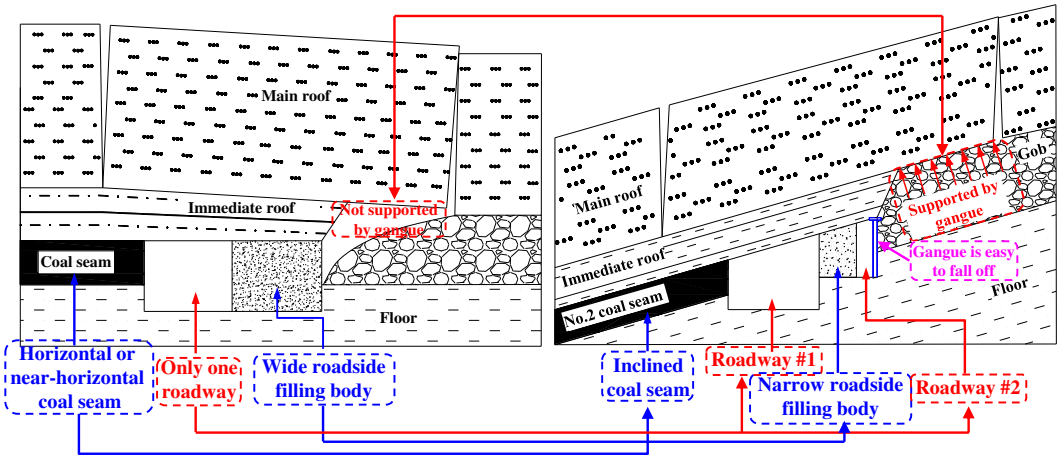

(a) Traditional gob-side entry retaining (b) Gob-side entry retaining in Zuozegou mine

Fig. 1 Comparison between the traditional GER and the GER with double roadways in Zuozegou mine

2. Engineering Geology

2.1. Geological overview of 2202 working face

Zuozegou mine is located to the southwest of Jinzhong County, Shanxi Province, China. It mainly mines No. 2 coal seam with an average buried depth of about 670 m. Working face 2202 is located in the south of No. 2 coal mining area with F_2 fault protective coal pillar in the south. The surface of 2202 working face is located in Fanwang Village whose eastern part belongs to hills and valleys and has a good drainage condition. The dip angle of No. 2 coal seam is 14° ~ 23° and the average dip angle is 16°, and it belongs to gently inclined coal seam. The average thickness of the coal seam is 1.62 m and its consistent coefficient *f* is 2 to 3 with the bedding and joints relatively developed. The upper part of the coal seam is a pseudo-roof mudstone of 0-0.2 m; the immediate roof is carbonaceous mudstone of 1.95 m and the main roof is fine-grained sandstone of 6.02 m. The comprehensive histogram of coal and rock strata is shown in Fig. 2.

Rock stratum	Legend of rock column	Thickness /m	Lithology description
Sandy mudstone		12.95	Dark gray, layered, evenly jointed, rich in plant fossil fragments, brittle and semi-hard, flat section
Fine-grained sandstone		6.02	Deep gray, layered, fissure developed, containing plant rhizome fossils
Carbonaceous mudstone		1.95	Argillaceous structure, angular fracture, local interbedding with siltstone, undeveloped bedding
No.2 coal seam		**1.62**	Black, massive, vitrinite-dominated, heterogeneous fracture, endogenous and exogenous fracture
Mudstone		3.05	Gray, flat fracture, horizontal and gentle wave bedding, siliceous cementation
Siltstone		4.50	Light gray and dark gray, medium thick layered, horizontal bedding and wavy texture
Mudstone		2.04	Gray, flat fracture, horizontal and gentle wave bedding, siliceous cementation

Fig. 2 Coal and rock strata histogram

The inclination length of 2202 working face is 180 m, and the tendency length is 1300 m. The mining method of 2202 working face is strike longwall comprehensive mechanized mining. The headgate of 2202 working face is excavated along the roof of No.2 coal seam, which is reserved by the method of GER for the next working face with a net cross section of 4.2×2.9 m (width × middle height).

2.2. Support scheme of 2202 headgate

Roof bolts for headgate are Φ20×2000 mm threaded steel resin bolts whose anchorage capacity is not less than 70 kN and pre-tightening torque is 150 N·m or more with the row and line space of 800 mm×800 mm. Bolts in two sides of the headgate are Φ16×2000 mm threaded steel resin bolts whose anchorage capacity is not less than 50 kN and pre-tightening torque is 120 N·m or more with the row and line space of 800 mm×800 mm. The anchor cables in both sides and the roof are Φ17.8×6000 mm steel strand with a pre-tightening force of 125 kN or more and a 300×300 ×20 mm square pallet. Two anchor cables shall be arranged in the middle roof with a spacing of 1600×1600 mm. Anchor cables in right side of the headgate shall be arranged with the row and line space of 1600 mm. The headgate support in 2202 working face is shown in Fig. 3.

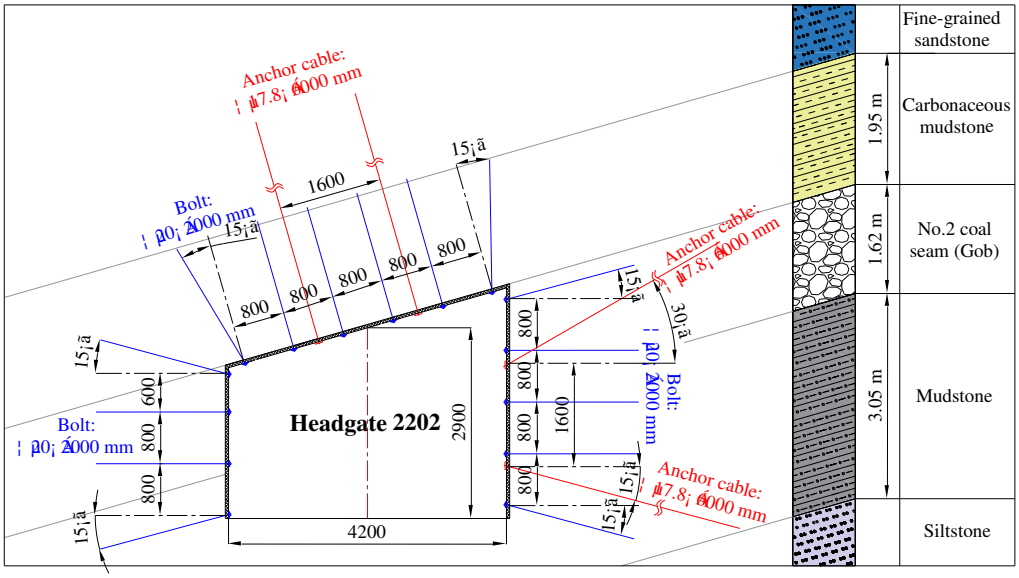

Fig. 3 Supporting diagram of the headgate

3. Basic properties of roadside high-water material

In order to ascertain the basic mechanical properties of roadside high-water material in the GER of 2202 working face in Zuozegou mine, multiple laboratory tests are used to study the main composition, micromorphology, stress-strain relationship, the connection among elastic modulus, peak stress and curing ages. It provides a theoretical basis for the application of high-water material in roadside filling of GER.

3.1. Basic composition and micromorphology of high-water material

High-water material (Xia et al. 2018) is a new hydraulic material composed of two main materials of A and B, two auxiliary materials of AA and BB, and the water. The XRD pattern of high-water material (Fig. 4) and the main ingredients of A and B (Table 1) are obtained by laboratory tests. It can be seen that the main component of material A is sulpho-aluminate cement and calcium silicate while B is anhydrite and quicklime. Materials AA and BB are auxiliary of materials A and B respectively, which are composite accelerator composed by accelerator and suspension dispersant.

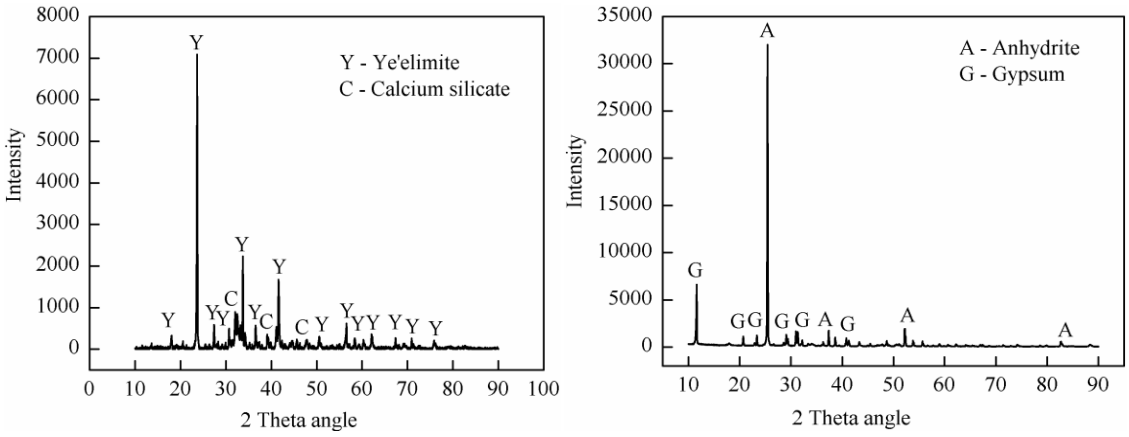

(a) Material A (b) Material B

Fig. 4 The XRD pattern of high-water material

Table 1 Comparison of chemical composition of materials A and B in high-water material (%)

	Yeelimite	Calcium silicate	Anhydrite	Gypsum
A	68.15	31.85	0	0
B	0	0	74.85	25.15

The configuration of high-water material is to mix materials A and AA, B and BB with water respectively to make slurries A and B through preparation system. The water should be added into AA and BB materials to make slurries active, and then added to the preparation of slurries A and B. The slurries of high-water material A and B are used together in a ratio of 1:1. The water-cement ratio of high-water material in roadside filling of GER in Zuozegou mine is 1.6:1. After two slurries are fully mixed, it quickly sets and hardens. It can be processed to form a standard specimen of high-water material with a certain strength, as shown in Fig. 5.

Fig. 5 Preparation process of standard specimens of high-water material

The micromorphology of high-water material with a water-cement ratio of 1.6:1 after the magnification of 1000 times, 2000 times, and 3000 times is shown in Fig. 6 by a laboratory CT (Computed Tomography) scanner. The hydration product of high-water material is mainly ettringite (molecular formula is $3CaO{\cdot}Al_2O_3{\cdot}3CaSO_4{\cdot}32H_2O$), and its microscopic morphology is mostly slender needle-like crystals with small crystal diameters. Its stone body is mainly composed of fine branch net structure, and each branch and column is overlapped and staggered with disordered arrangement. The distance between the branches and columns is obvious and the gap is large. The massive structure is calcium carbonate and its distribution is relatively concentrated, part of which forms a certain overall structure. Micro-pores are developed in the surface microstructure. The branches and columns of the stone body are relatively compact due to the fact that the low water content of roadside high-water material in Zuozegou mine.

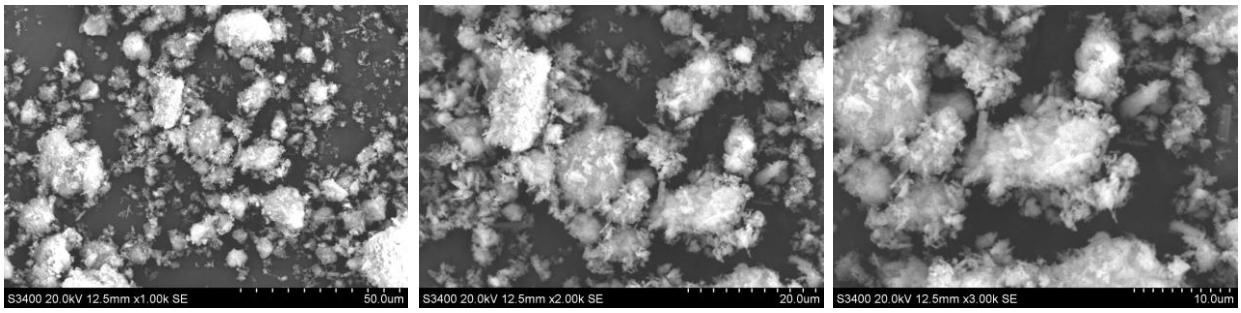

(a) Magnification of 1000 times (b) Magnification of 2000 times (c) Magnification of 3000 times

Fig. 6 Morphological characteristics of high-water material with a water-cement ratio of 1.6:1

3.2. Characteristics of stress-strain relationship of high-water material

By preparing Φ50×100 mm standard cylindrical specimens of high-water material with a water-cement ratio of 1.6:1 in the laboratory, the standard specimens within 1-day, 3-day, 7-day and 28-day curing are subjected to uniaxial compressive strength tests. At least 3 standard specimens should be made for each curing age and the surface should be covered after the test specimens are completed. The standard specimens of high-water material are regularly cured in a constant temperature and humid environment and the uniaxial compressive strength test should be conducted for

the specimens cured for a certain age. The laboratory test results are shown in Fig. 7.

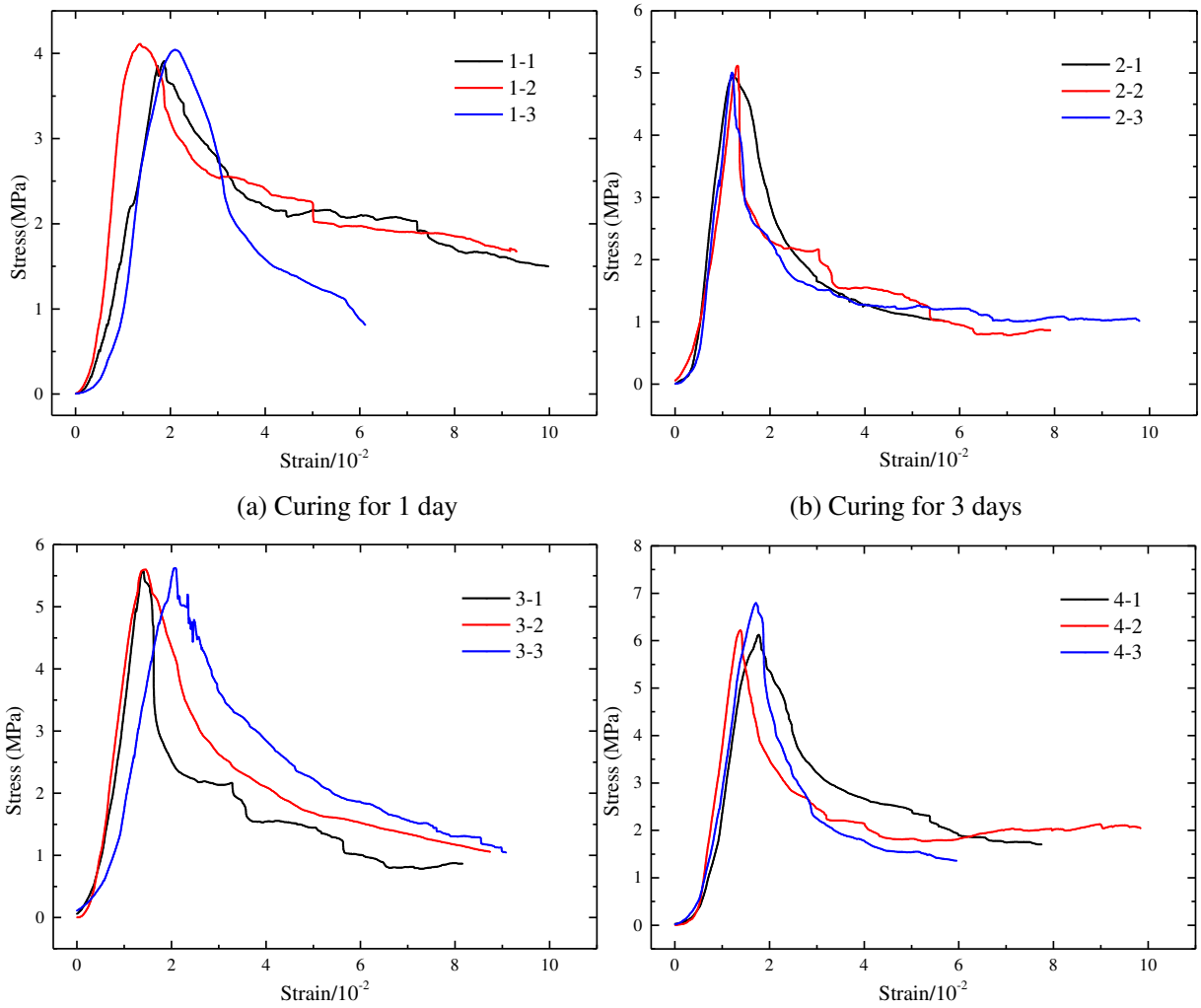

Fig. 7 Strength curves of high-water material for different curing ages

The uniaxial compressive strength tests of high-water material for different curing ages show that: ①The high-water material has moderate strength and high shrinkage at the initial stage of curing and can adapt to the deformation movement of the overlying main roof in the retained roadway, which plays a role of yielding pressure. ② The high-water material has obvious plastic characteristics. The stress slowly decreases and tends to a stable value as the strain continues to increase after the peak stress of high-water material, which means it still has a certain bearing capacity after plastic failure. This is essentially different from brittle materials such as rocks and coal bodies. ③The peak compressive strength of high-water material increases significantly with the extension of curing ages while it still presents obvious plastic failure characteristic.

Fig. 8 shows the average peak compressive strength and elastic modulus of high-water material for different curing ages. The peak compressive strength is 4.03 MPa after curing for 1 day, and its elastic modulus is 400 MPa. The peak strength and elastic modulus increase rapidly after curing for 3 days and increase to 5.03 MPa and 580 MPa, respectively. After curing for 7 days, the peak strength and elastic modulus are 5.60 MPa and 641 MPa, respectively. When the curing age increases to 28 days, The peak strength and elastic modulus increase to 6.39 MPa and 824 MPa, respectively. Therefore, the peak compressive strength and elastic modulus of high-water material are both growing up with the increase of curing ages. The strength of high-water material with a water-cement ratio of 1.6:1 reaches to 6.39 MPa after curing for 28 days. The elastic modulus of high-water material within 1-day, 3-day, 7-day and 28-day

curing are 400 MPa, 580 MPa, 641 MPa and 824 MPa, respectively. The fitting curve of the relationship between elastic modulus and curing age is y=822.70-471.23×0.85^x, and the goodness of fit R^2 is 0.96.

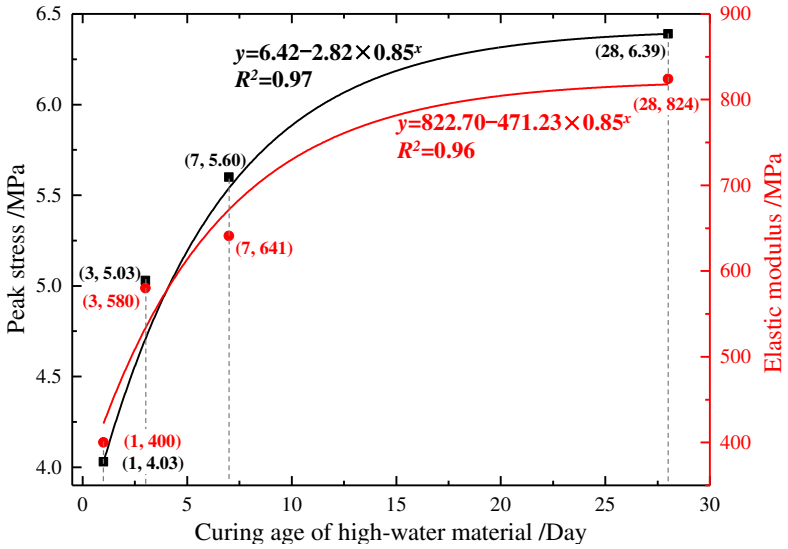

Fig. 8 Curves of peak compressive strength, elastic modulus and curing age of high-water material

In conclusion, the peak strength of roadside high-water material of 2202 working face in Zuozegou mine with a water-cement ratio of 1.6:1 can reach 6.39 MPa and the elastic modulus is 824 MPa after curing for 28 days. Therefore, as a new type of filling material, high-water material has many advantages such as quick solidification, stable performance, obvious plastic characteristic, low cost and certain flexibility to adapt to the large deformation of surrounding rock, which has been tested and widely used in various coal mines in China.

4. Width determination of roadside filling body of GER with double roadways

According to the surrounding rock force of GER and the breaking characteristics of the main roof, the simplified mechanical model of the interaction between roadside support and roof strata is shown in Fig. 9.

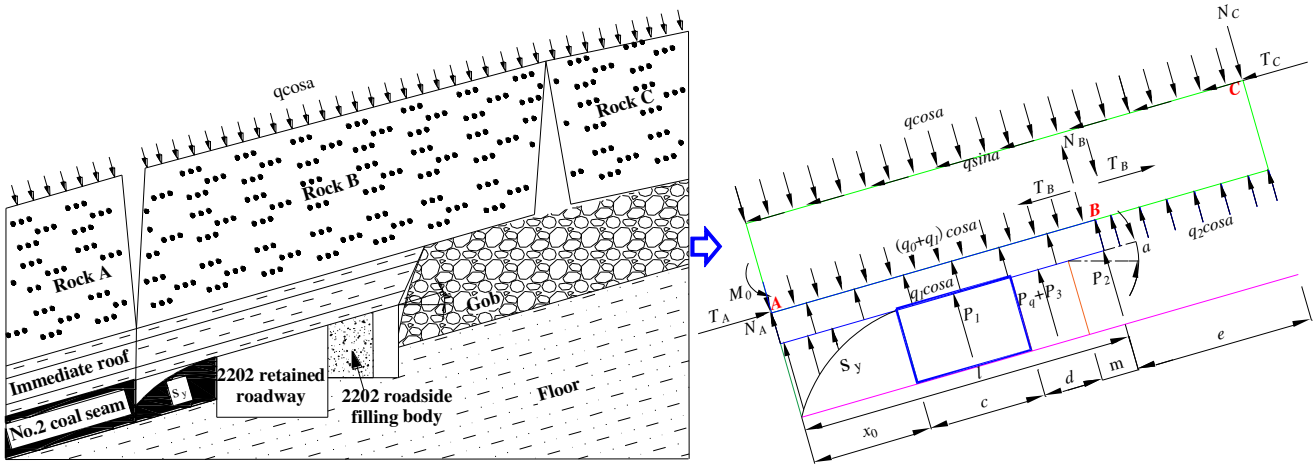

Fig. 9 Mechanical model of GER with double roadways in gently inclined coal seam

In the above mechanical model of GER with double roadways in gently inclined coal seam, the formula of the limit equilibrium zone (Huang et al. 2018) in solid coal side is

$$x_0 = \frac{mA}{2\tan\varphi_0}\ln\left[\frac{k\gamma H + \frac{c_0}{\tan\varphi_0}}{\frac{c_0}{\tan\varphi_0} + \frac{p_x}{A}}\right] \tag{1}$$

In formula (1), x_0 is the limit equilibrium zone in solid coal side, m; m is the mining height, 1.62 m; A is the coefficient of lateral pressure, 1.2; H is the mining depth, 670 m; c_0 is the cohesion force, 0.9 MPa; φ_0 is the internal friction angle of the coal, 32°; k is the maximum stress concentration factor, 2.7; γ is the average weight of overlying rock strata, 25 kN/m^3; p_x is the support strength in solid coal, 0.28 MPa. It can be calculated that the limit equilibrium zone x_0 is 5.17 m.

In Fig. 9, the mechanical equilibrium equation of surrounding rock structure of GER in gently inclined coal seam is

$$\begin{cases} q\cos\alpha\dfrac{(l+e)^2}{2} - q\sin\alpha(l+e)h - N_C(l+e) - q_1\cos\alpha\dfrac{l^2}{2} - q_2\cos\alpha e(l+\dfrac{e}{2}) - \mathrm{T}_C(h-\Delta S_B) = 0 \\ q\cos\alpha(l+e) + N_C - q_2\cos\alpha e - N_A - q_1\cos\alpha l = 0 \\ (q_0+q_1)\cos\alpha\dfrac{l^2}{2} - M_0 - \int_0^{x_0}\sigma_y(x_0-x)dx - P_1(x_0+\dfrac{c}{2}) - (P_q+P_3)(x_0+c+\dfrac{d}{2}) - P_2 l = 0 \end{cases} \tag{2}$$

In formula (2), σ_y is the support force of coal in the limit equilibrium zone, kN/m^2; P_q is the support resistance of roadside high-water material, kN/m; P_1 is the support resistance of single props in GER, kN/m; P_2 is the support resistance of single props in the outer roadway of GER, kN/m; P_3 is the support resistance of single props on both sides of roadside filling body, kN/m; q_2 is the support force of gangue to rock B, kN/m^2 ; N_C is the shear of rock C to rock B, kN/m; N_A is the shear of rock A to rock B, kN/m; q is the load of the main roof and overlying soft rock strata, kN/m^2; l is the contact length between the immediate roof and the main roof, m, which can be expressed as $l=x_0+c+d+m$; e is the suspension length of rock B behind the working face, m; q_0 is the weight of the immediate roof, kN/m^2; q_1 is the force of the immediate roof (main roof) to the main roof (immediate roof), kN/m^2; T_C is the thrust of rock C to rock B, kN/m; h is the thickness of the main roof, m; ΔS_B is the right sinking amount when rock B rotates at a certain angle, m; M_0 is the residual bending moment of the immediate roof, kN·m.

The calculation formula of the suspension length e of rock B is

$$e = \frac{2b}{17}\cdot\frac{b}{L_m}\cdot\sqrt{100+102(\frac{L_m}{b})^2} - x_0 - c - d \tag{3}$$

In formula (3), b is the weighting step of the main roof, m; L_m is the length of 2202 working face, m.

According to formulas (2)~(3), combined with the observation results of 2202 working face and its various parameters: α=16°; x_0=5.17 m; e=13.92 m; N_C=0; N_A=0; $P_1=P_3$=360 kN/m; P_2=180 kN/m; q=903 kN/m^2; q_0= 48.75 kN/m^2; q_2=14.76 kN/m^2; h=6.02 m; c=4.2 m; d=1.8 m; m=1.0 m; l=12.17 m; b=21 m; L_m=180 m; T_C=2157.60 kN/m; ΔS_B=0.79 m; M_0=0. It is calculated that the support resistance to be provided for roadside high-water material of GER in Zuozegou mine is 10.24 kN/m. It can be seen from the advancement of 2202 working face and the filling process of high-water material that roadside single props need to be safely recovered after 9 days. As can be seen from Fig.8, the peak compressive strength of roadside high-water material is 5.82 MPa after curing for 9 days. Combined with the calculation formula of roadside supporting width, the roadside width of high-water material should not be less than 1.76 m. Then the width of roadside high-water material is determined to be 1.8 m and the width-to-height ratio is greater than 0.6, which satisfies the roadside supporting stability of GER.

5. Stability characteristics of surrounding rock of GER

In order to study the failure characteristics of surrounding rock of GER, a numerical calculation model is constructed to study the distribution characteristics of vertical stress and plastic zone when the roadway is undisturbed by 2202 working face and stabilized after the mining. It provides a basis for formulating the control scheme of surrounding rock of GER.

5.1. Numerical model

According to the geological conditions of Zuozegou mine, the FLAC^{3D} simulation software is used to establish a numerical model of GER in 2202 working face, as shown in Fig. 10. In the model, the dip of 2202 working face is taken as 110 m, and the advancement is taken as 160 m and the vertical direction of the model is taken as 140 m. Number of Gps and zones are 821583 and 787680, respectively.

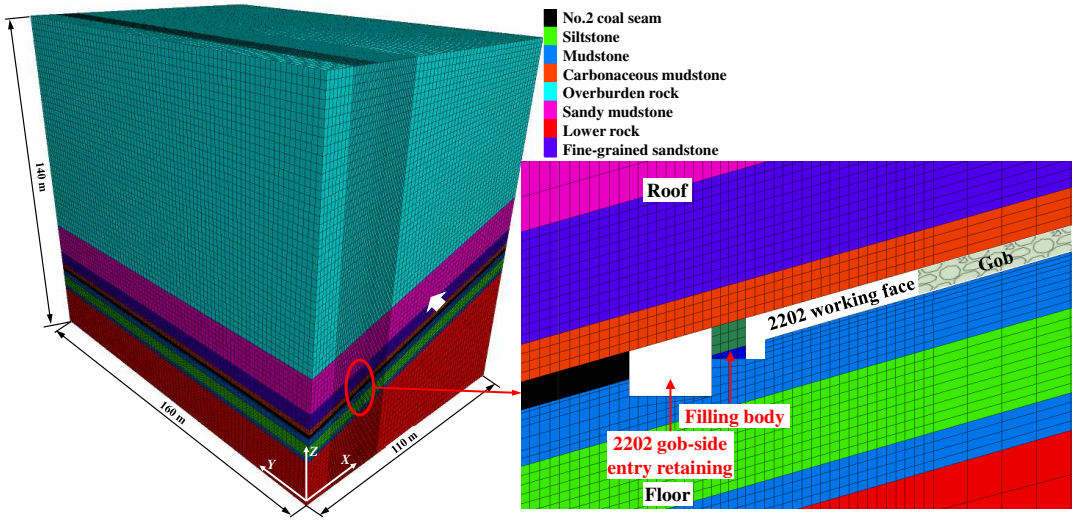

Fig. 10 Numerical model

The constitutive relationship of each rock stratum adopted in the model is the Mohr-Coulomb criterion (Yu and Liu 2018; Wang et al. 2020), and roadside high-water material is a nonlinear strain-softening model, and the goaf is the double-yield model (Li et al. 2015). The physical and mechanical parameters of each coal and rock stratum in the model are shown in Table 2.

Table 2 Mechanical parameters of each coal and rock stratum

Lithology	Bulk modulus (GPa)	Shear modulus (GPa)	Cohesion (MPa)	Tensile strength (MPa)	Internal friction angle (°)	Density (g/cm^3)
Sandy mudstone	2.48	2.02	1.97	1.32	24	2.34
Fine-grained sandstone	5.69	2.91	2.32	1.92	29	2.66
Carbonaceous mudstone	2.33	1.91	1.90	1.23	23	2.01
NO.2 Coal seam	2.28	1.58	1.27	1.13	21	1.35
Mudstone	2.31	1.88	1.86	1.21	22	13
Siltstone	4.98	3.54	2.69	2.17	30	2.75

5.1.1. Mechanical parameters of nonlinear strain-softening model

Strain-softening (Zhang et al. 2017), which means the stress quickly decreases to a smaller stable value after it reaches the peak as the strain continues to increase while still has a certain bearing capacity. From the uniaxial compression stress-strain curves of high-water material in Fig. 7, we can see that the stress decreases and tends to a stable value as the strain continues to increase after the peak strength of high-water material. At this time, the high-water material still has a certain bearing capacity. Therefore, the failure process of high-water material is more in line with the strain-softening model, which is mainly based on the Mohr-Coulomb yield criterion.

The strain-softening parameters ε, φ of roadside high-water material of GER and C of the coal are obtained

through laboratory experiments, as shown in Table 3.

Table 3 Parameters of cohesion and friction angle with the change of plastic strain

ε	φ (°)	C (MPa)
0	21.0	0.79
0.017	17.0	0.54
0.021	13.0	0.31
0.026	11.0	0.22

5.1.2. Mechanical parameters of double-yield model

The roof above the goaf collapses and is gradually compacted after the mining of 2202 working face. The modulus after compaction increases significantly. The collapsed goaf not only has to bear part of the roof load, but also affects the stress distribution of the floor. Therefore, the double-yield model is used to simulate the strain of the goaf, and the maximum strain and initial modulus of the goaf in FLAC^{3D} are calculated by the Salamon equation to be 0.23 and 16.26 MPa, respectively. The cap pressures used in the double-yield model are listed in Table 4.

Table 4 The cap pressures of the double-yield model

Strain	Stress (MPa)	Strain	Stress (MPa)
0.01	0.14	0.11	3.27
0.02	0.29	0.12	3.88
0.03	0.50	0.13	4.59
0.04	0.71	0.14	5.24
0.05	0.98	0.15	6.74
0.06	1.16	0.16	8.28
0.07	1.43	0.17	10.12
0.08	1.83	0.18	12.97
0.09	2.25	0.19	16.85
0.10	2.69	0.20	22.46

The material parameters of the double-yield model in FLAC^{3D} are shown in Table 5.

Table 5 Material parameters of the double-yield model

Parameter	D(kg·m^{-3})	K(GPa)	G(GPa)	φ_m(°)	Dilation(°)
Value	1040	1.17	0.48	18	6

5.2. Stability analysis of GER with double roadways

In this section, the FLAC^{3D} numerical calculation software is used to simulate the distribution characteristics of vertical stress and plastic zone of surrounding rock when the headgate is not disturbed and affected stably by the mining of 2202 working face (Fig. 11). The vertical stress of the roof and two sides of the roadway is extracted through the nephogram to analyze the failure characteristics of surrounding rock of GER.

From the distribution curves of vertical stress of the roadway in Fig. 11a and Fig. 11b, it can be seen that the peak stress in solid coal increases from 22.15 MPa when the headgate is not disturbed to 43.85 MPa after mining stability of 2202 working face. The stress concentration factor increases from 1.32 to 2.62 and the peak distance increases from 2.50 m to 4.40 m. The peak stress is obviously increased and moves to the deeper affected by the mining disturbance. When the coal in mining side is not affected by the mining disturbance, the peak stress is about 22.49 MPa and the stress concentration factor is 1.34 and the peak distance is 3.0 m which are slightly larger than in solid coal side. After the mining of 2202 working face, roadside high-water material is filled and the stress of 1.8-m-wide high-water material is low. The vertical stress in the filling body is approximately symmetrical with the peak stress of 5.89 MPa after the stability of mining disturbance. Fig. 8 reveals that the peak compressive strength of high-water material after curing for 28 days can reach to 6.39 MPa with extremely strong plastic characteristics. Therefore, roadside high-water material can effectively bear the roof load after the stability of mining disturbance.

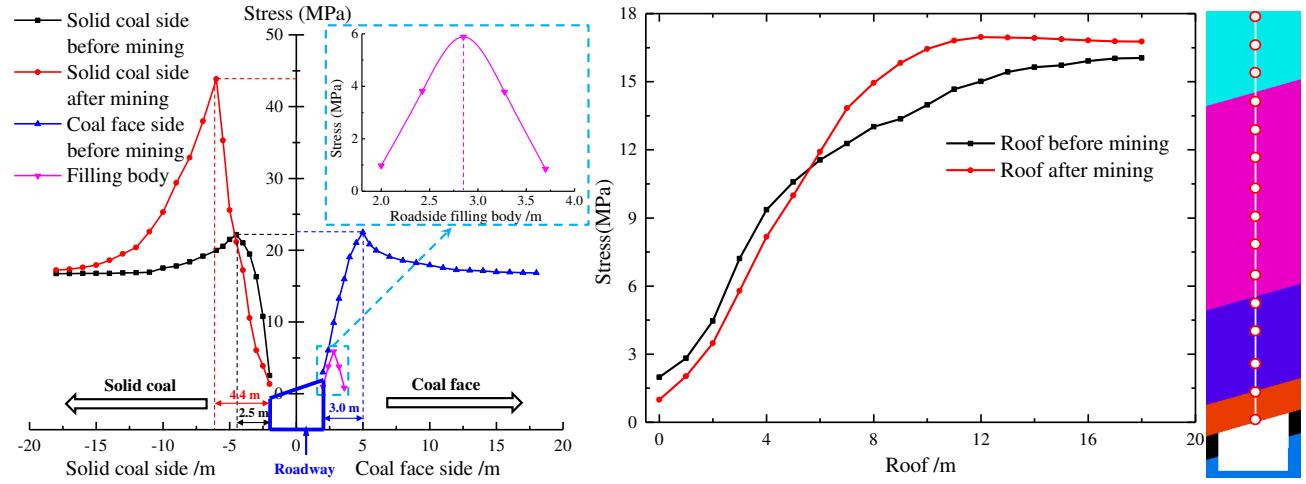

(a) Two sides of the roadway

(b) Roadway roof

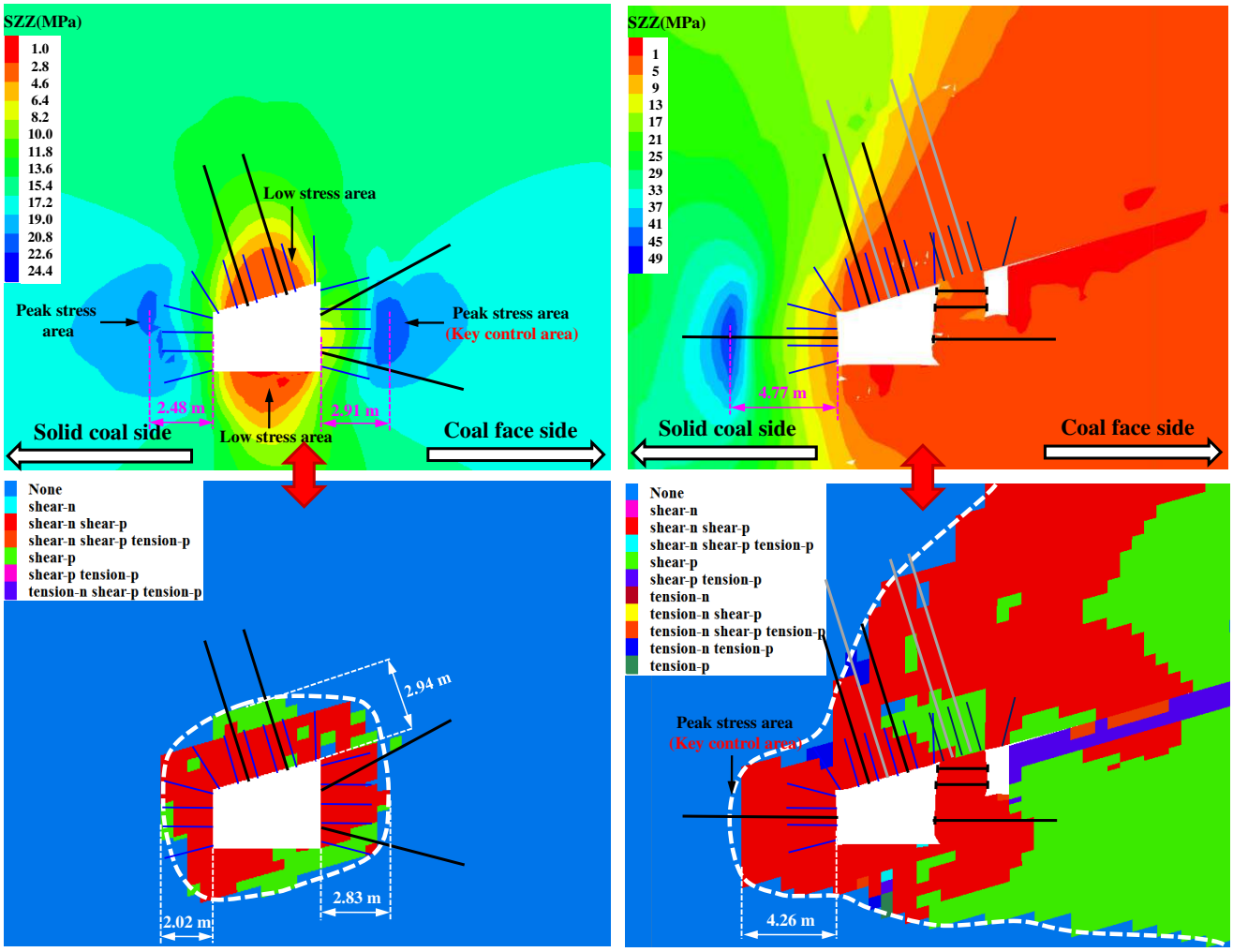

(c) The headgate

(d) Retained roadway

Fig. 11 Vertical stress and plastic zone distribution of roadway surrounding rock

It can be seen from Fig. 11c that the peak zone of the roadway stress is mainly distributed in two sides when the headgate is excavated and not affected by the mining of 2202 working face. The peak distances in solid coal side and mining side are 2.48 m and 2.91 m, respectively. The surrounding rock in the shallow roof is in a failure state with a low stress value, which is the key control area of surrounding rock of the roadway. Before the mining disturbance of

2202 working face, the plastic zone ranges of the roadway roof, solid coal and mining side are 2.94 m, 2.48 m, and 2.83 m, respectively, which are the same as the vertical stress distribution of the roadway approximately. The surrounding rock in the shallow of the roadway is mainly shear and tensile failure. After the mining of 2202 working face, the peak stress zone of surrounding rock of the retained roadway is mainly distributed at 4.77 m from solid coal with a peak stress value of 46.37 MPa, as shown in Fig. 11d. The immediate roof occurs collapse and the main roof occurs periodic breakage under the mining disturbance (Wang et al. 2019a; Wang et al. 2019b). The roof and floor near the gob side are in a low stress state on a large scale. Although roadside high-water material is completely in a plastic state, the deformation of filling body is not large and it still has a strong bearing capacity (Tan et al. 2015; Yu et al. 2019; Xie et al. 2020). The plastic range in solid coal side of the retained roadway is 4.26 m, which is approximately consistent with the distribution of the vertical stress.

In summary, the surrounding rock deformation of 2202 GER increases sharply under the mining disturbance of 2202 working face. The peak stress in solid coal of the roadway increases and moves to the deeper obviously. The peak stress distance and plastic zone range in solid coal side are 4.0 m and 3.86 m, respectively. The shallow of the retained roadway roof is in a low-stress state with large plastic zone, and its goaf roof is in a plastic failure state. Roadside filling body of high-water material is always in plastic state with a peak stress of 5.89 MPa. In view of this, it is necessary to ensure that the anchor cables pass through the shallow plastically damaged surrounding rock and anchor into the deep stable rock of the retained roadway.

6. Engineering Application

Based on the failure range of surrounding rock of GER of 2202 working face in Zuozegou mine, a coupling control technology of anchor cables and bolts in the roof and solid coal + single props in entry-in support and goaf side of the outer roadway + anchor bolts in roadside high-water material + short anchor cables below the filling body is proposed and conducted in industrial test. The reinforcement effects of GER are verified by coupling methods of arranging borehole peeping, observing the convergences and measuring the load of the filling body.

6.1. Filling process of roadside high-water material in GER

In order to ensure that two parts of high-water material are not solidified during the transportation process, it is necessary to add water and stir separately using a mixing tank. The dual-liquid filling pump pressurizes two slurries separately, and the double-pass high-pressure pipeline conveys the slurries into the filling bag and then needs to be mixed and solidified. The filling procedure of high-water material of GER in 2202 working face is shown in Fig. 12.

The anchor bolts are passed through the filling bag and connected to the U-shaped steel, and the single props in two sides of roadside filling body are fastened. The special person checks that all works are ready before the pump is started. The mixing tube should be inserted into the filling bag for formal filling after observing the slurries flowing out of the discharge port uniformly. When the mixture is about to connect the roof, close observation should be made to ensure the filling bag is tight to the roof without leaving gaps. Once the roof connection is successful, the grouting tube should be taken out of the filling bag immediately and a signal should be sent to stop grouting immediately, and the filling port should be firmed with a rope to prevent the slurries from overflowing. At the same time, the staff at filling station should quickly open the water valve to rinse the mixing pipe to avoid being blocked. At the end of the filling work, the pumping station should be notified immediately to clean the pipeline by clear water.

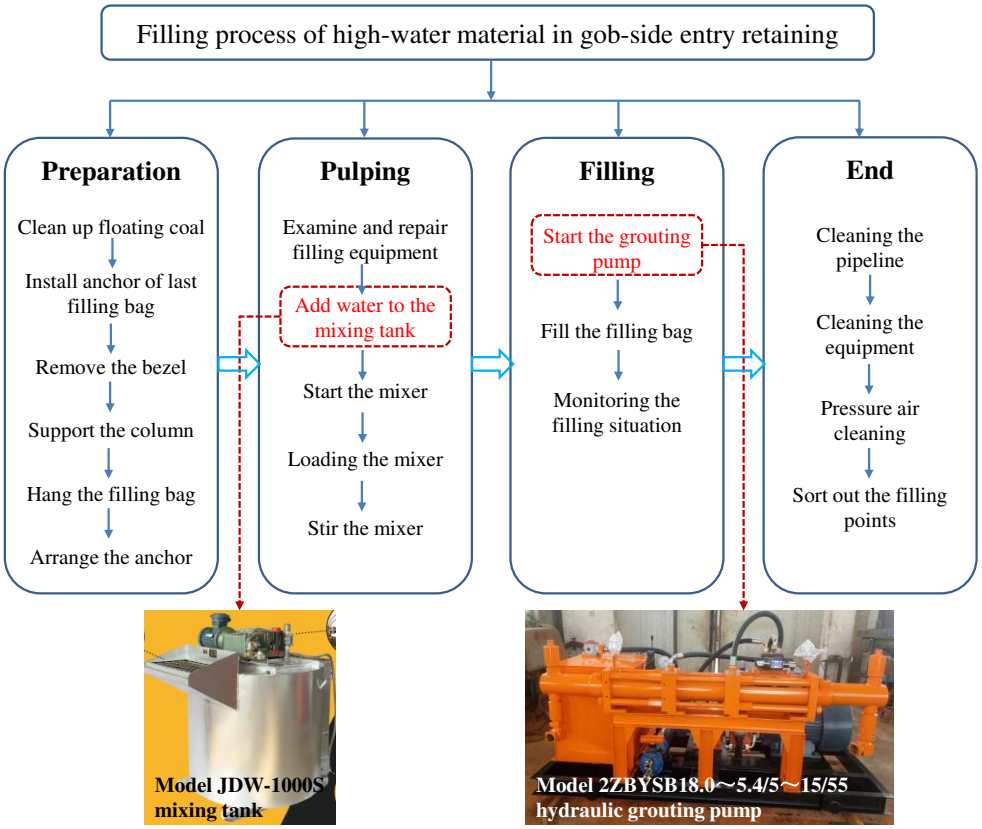

Fig. 12 Filling procedure of high-water material of GER

6.2. Supporting parameters of surrounding rock of GER

(1) Roof support: A row of Φ21.6×8000 mm anchor cables are arranged along the roof center of GER, and the row and line space is 0.8×1.6 m. The matching square plate is 300×300×20 mm with a pre-tightening force of 250 kN or more. At the same time, two rows of single props are used to support the roadway roof with the row and line space of 1400×500 mm.

(2) Solid coal support: A row of Φ21.6×6000 mm anchor cables are arranged in solid coal side with a row spacing of 1.6 m. Cables are anchored by CK2335 and Z2360 anchoring agents and connected together with steel ladder beams. The matching square plate is 300×300×20 mm with a pre-tightening force of 250 kN or more.

(3) Support of expanding brush section: In order to ensure the filling construction safety, the filling bag area in front of the support should be expanded in advance with a size of 3.6×2.8 m. The expanded roof is supported by bolts and anchor cables. The Φ21.6×8000 mm anchor cables are arranged perpendicularly to the roof strata with the row and line space of 800×1600 mm. Four Φ20×2000 mm threaded steel bolts are arranged in each row of the roof. The row spacing of the bolts above the filling body is 800 mm while the gob side is 1000 mm. The matching square plate is 150×150×10 mm with an anchorage capacity not less than 70 kN and a pre-tightening force of 150 kN or more.

The metal net with the specification of 2.8×1.2 m is laied on the roof of the expanded area. Two rows of cutting props should be erected in time with the articulated roof beam in the filling area near the gob side, and the row spacing is 1.0 m. U-shaped steel and single props are separately supported in both sides of the filling bag with the row spacing of 0.4 m, and the steel is connected by two sections of 1.2-m-long cables to adapt to different heights of the roof. At the same time, in order to enhance the stability of roadside high-water material, the Φ20×2200 mm threaded steel anchor bolts are arranged to punch both sides of the U-shaped steel with the row spacing of 800 mm. The nuts are processed on both ends of the anchor bolts which are matched with the specifications of 150×150×10 mm (length × width × thickness) plates. The upper and lower anchor bolts are vertically connected together by a ladder beam.

There is a 1-m-wide working space between the filling body of GER and the gob. In order to prevent the gangue from entering into the outer roadway, the semi-circular timbers should be mounted when the single props are erected near the gob side with a spacing of 1 m, which can form a partition wall of gangue group. The supporting scheme of GER with double roadways by filling with 1.8-m-wide high-water material is shown in Fig. 13.

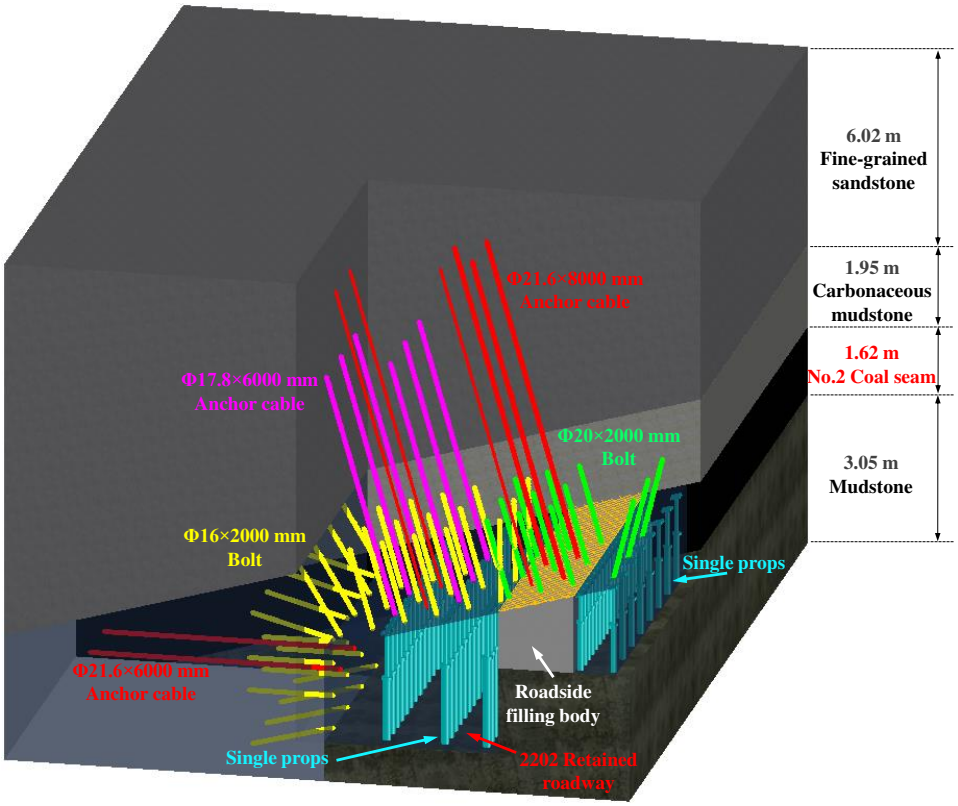

(a) Schematic diagram of three-dimensional support

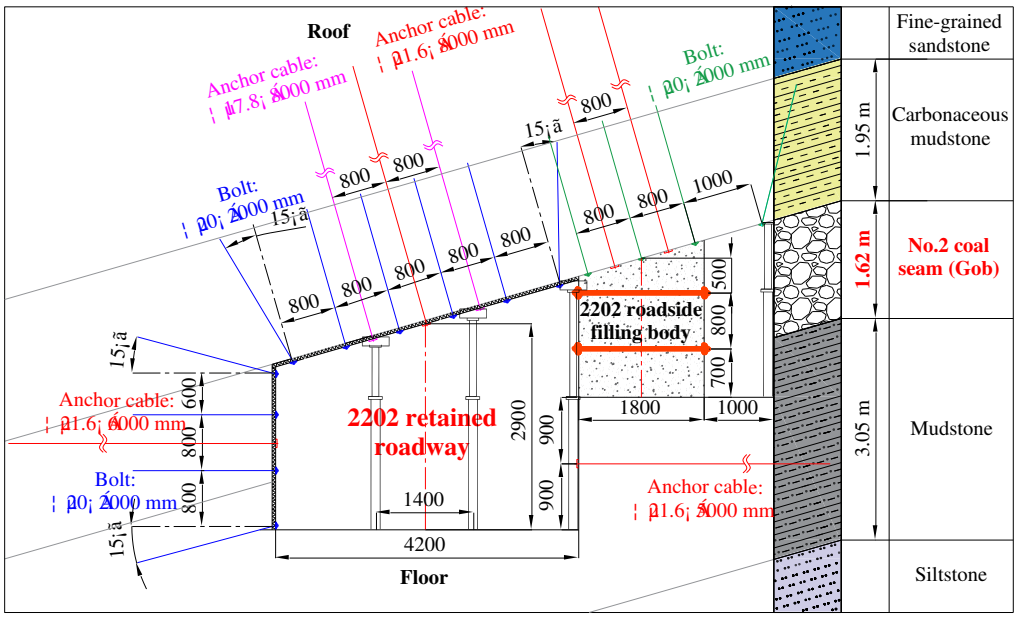

(b) Schematic diagram of supporting plane

Fig. 13 Supporting scheme of 2202 GER

6.3. Results and analysis of mine pressure observation

6.3.1. Results and analysis of borehole peeping

The ZKXG100 mine-used borehole imaging and trajectory detection (Fig. 14a) is a comprehensive device particularly suitable for underground coal mine detection. It can be configured as a drilling peeping to perform full-hole imaging and recording of various boreholes (Fig. 14b). It is used to observe the geological structural characteristics such as the occurrence, development and the separation degree of coal seam cracks in the borehole (Wang et al. 2018; Xie et al. 2019). It can also distinguish various geological structures such as rock mass, coal seam and gangue.

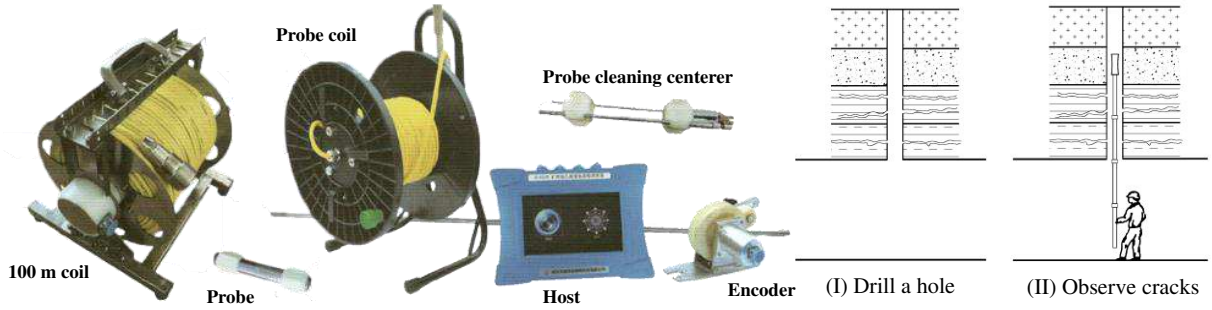

(a) ZKXG100 borehole imaging and trajectory detection (b) Sketch map of borehole peeping

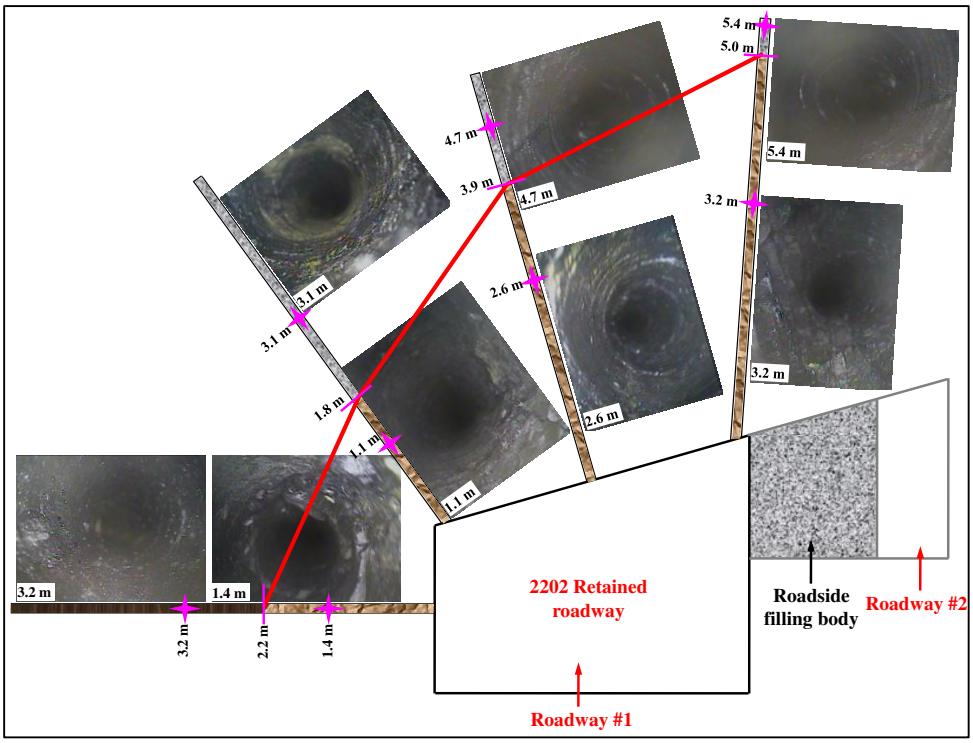

(c) Drilling peeping results

Fig. 14 Principles and results of drilling peeping

In order to verify the control effects of surrounding rock of GER in 2202 working face, the ZKXG100 mine-used borehole imaging and trajectory detection is used to observe the structure, and the peeping effects are shown in Fig. 14c. The results show that coal body is relatively fragmented with many irregular and large fractures within 2.2 m of the initial entrance hole in solid coal side of the retained roadway. There is no large fracture found and the integrity is good as the depth greater than 2.2 m. Rock mass fissures are well developed in the range of 3.9 m perpendicular to the roadway roof with large fracture apertures. The rock mass integrity is poor which is prone to collapse. The fractures in rock mass are significantly reduced and the number is almost 0 as the depth greater than 3.9 m. The loosening damage ranges of the roof angle in solid coal side and gob side are 1.8 m and 5.0 m, respectively. There are many small

horizontal, vertical and irregular cracks and joints distributed in the rock mass, and the rock mass gradually becomes more complete beyond this range. Therefore, it is verified by borehole peeping that the long anchor cables have passed through the loosening failure zone in the shallow of the retained roadway, and the supporting effect of surrounding rock of GER is remarkable.

6.3.2. Results and analysis of surrounding rock convergences and filling body load

In order to analyze the failure characteristics of surrounding rock of GER after the coupling control technology, the roof-floor convergence, the relative maximum convergence of two sides and the load of filling body should be used as the observation indicators (Fig. 15a). Observation stations are arranged in the roadway to get the deformation of surrounding rock and the load of hydraulic pillows embedded in the filling body, which can provide a basis for evaluating the control effects of surrounding rock. The observation results of roof-floor convergence, two sides convergence of GER and the load of filling body are shown in Fig. 15b. The roof-floor and two sides convergences and the load of filling body increase rapidly after the mining of 2202 working face. After advancing 60 m of the working face, the relative moving speeds of two sides and roof-floor, the load increasing speed of roadside filling body gradually slow down. However, the convergences of surrounding rock and the loads of the filling body still present a slow growth trend. After advancing 80 m of the working face, the convergence of surrounding rock and the load of the filling body of GER don't increase almostly. At this time, the convergences of two sides and the roof-floor are stabilized at 252 mm and 269 mm separately, and the load of the filling body is 5.54 MPa. There is no damage to the supporting system such as bolts and anchor cables and the GER by filling with 1.8-m-wide high-water material under the mining disturbance meets the actual production needs of the mine. Therefore, the coupling control technology achieves effective control of surrounding rock deformation of the retained roadway.

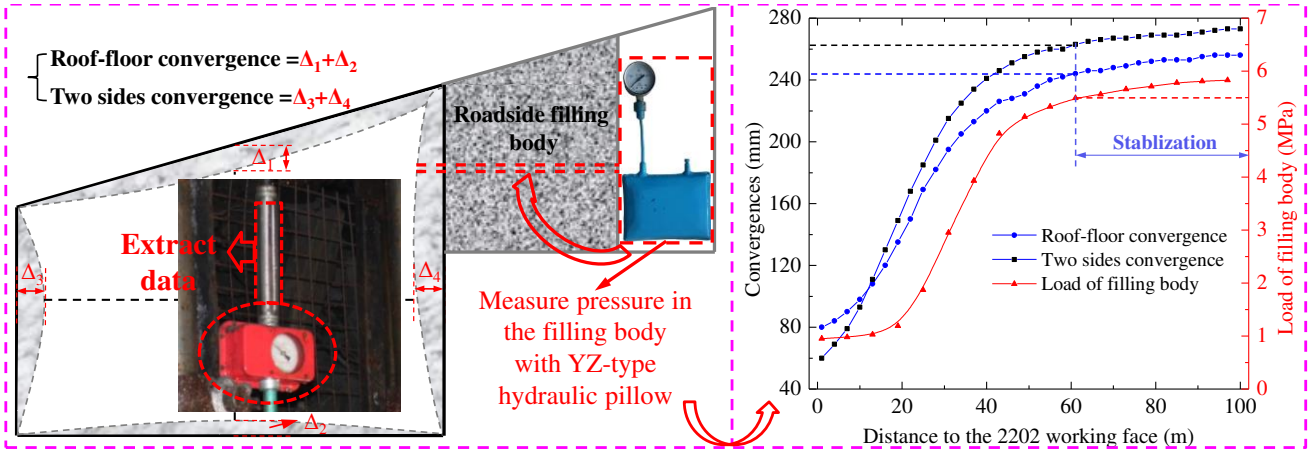

(a) Schematic diagram of mine pressure observation (b) Observation curves of mine pressure

Fig. 15 Mine pressure curves of 2202 gob-side entry retaining

7. Conclusions

(1) The experimental results show that the main components of high-water material are sulpho-aluminate cement and calcium silicate, anhydrite and quicklime, and its hydration products are mainly calcium vanadium. The micro morphology of high-water material is mostly slender needle-like crystals with small crystal diameters, and the inside of the stone body is mainly composed of fine branch-like structures. The high-water material with a water-cement ratio of 1.6:1 has a uniaxial compressive strength of 6.39 MPa and an elastic modulus of 824 MPa. The fitting curve of the relationship between elastic modulus and curing age of high-water material is y=822.70-471.23×0.85x, and the goodness of fit R^2 is 0.96.

(2) It is determined that the width of roadside high-water material of GER with double roadways in gently inclined coal seam is 1.8 m, which is obtained from constructing a mechanical model of GER and combining the peak strength of high-water material.

(3) The numerical simulation results show that the peak stress in solid coal of GER increases and moves to the deeper obviously after the stability of mining disturbance. The peak distance of vertical stress and plastic zone of solid coal are 4.0 m and 3.86 m, respectively. The shallow of the GER roof is in a low-stress state, and the range of plastic zone is large. The peak stress of roadside high-water material is 5.89 MPa.

(4) Based on the damage range of surrounding rock of GER, a coupling control technology of anchor cables and bolts in the roof and solid coal + single props in entry-in support and goaf side of the outer roadway + anchor bolts in roadside high-water material + short anchor cables below the filling body is proposed. It can be concluded that the 2202 GER with double roadways has good control effect by field application and mine pressure observation. The research results of this paper provide a certain scientific basis for the popularization and application of high-water material for roadside filling of GER in coal mines.

Acknowledgements This work was financially supported by the National Natural Science Foundation of China (Grant No. 52074296, 52004286), the China Postdoctoral Science Foundation (Grant No. 2020T130701, 2019M650895). The authors would like to thank the continuous support from Zuozegou coal mine during the on-site sampling and monitoring. The authors are extremely grateful to the anonymous reviewers for taking valuable time from their busy schedules to provide invaluable suggestions and pertinent comments to improve this paper. The authors are also thankful for the support of the journal.

Declarations

Conflict of interest The authors declare that they have no known competing financial interests or personal relationships that could have appeared to influence the work reported in this paper.

Ethical approval The experiments comply with the current laws of China.

References

Bai JB, Zhou HQ, Hou CJ et al (2004) Development of support technology beside roadway in gob-side entry retaining for next sublevel. J China Univ Min Technol 33(2):59-62

Bai JB, Shen WL, Guo GL et al (2015) Roof deformation, failure characteristics, and preventive techniques of gob-side entry driving heading adjacent to the advancing working face. Rock Mech Rock Eng 48(6):2447-2458. https://doi.org/10.1007/s00603-015-0713-2

Feng XW, Zhang N (2015) Position-optimization on retained entry and backfilling wall in gob-side entry retaining techniques. Int J Coal Sci Technol 2(3):186–195. https://doi.org/10.1007/s40789-015-0077-y

He MC, Gao YB, Yang J et al (2017) An innovative approach for gob-side entry retaining in thick coal seam longwall mining, Energies 10(11):1785. https://doi.org/10.3390/en10111785

Huang YL, Zhang JX, Zhang J et al (2011) Technology of gob-side entry retaining on its original position in fully mechanized coalface with solid material backfilling. J Chin Coal Soc 36(10):1624-1628. doi:10.13225/j.cnki.jccs.2011.10.024

Huang WP, Gao YF, Wen ZJ et al (2015) Technology of gob-side entry retaining using concrete-filled steel tubular column as roadside supporting. J China Univ Min Technol 44(4):604-611. doi:10.13247/j.cnki.jcumt.000359

Huang BX, Liu JW, Zhang Q (2018) The reasonable breaking location of overhanging hard roof for directional hydraulic fracturing to control strong strata behaviors of gob-side entry. Int J Rock Mech Min Sci 103: 1-11. https://doi.org/10.1016/j.ijrmms.2018.01.013

Kang HP, Niu DL, Zhang Z et al (2010) Deformation characteristics of surrounding rock and supporting technology of gob-side entry retaining in deep coal mine. Chin J Rock Mech Eng 29(10):1977-1987

Kong DZ, Pu SJ, Cheng ZH et al (2021) Coordinated Deformation Mechanism of the Top Coal and Filling Body of Gob-Side Entry Retaining in a Fully Mechanized Caving Face. Int J Geomech 21(4):04021030. doi:10.1061/(ASCE)GM.1943-5622.0001972

Li XL, Liu CW (2018) Mechanical properties and damage constitutive model of high water material at different loading rates. Adv Eng Mater 20(6):1701098. https://doi.org/10.1002/adem.201701098

Li WF, Bai JB, Peng Syd et al (2015) Numerical modeling for yield pillar design: a case study. Rock Mech Rock Eng 48:305-318. https://doi.org/10.1007/s00603-013-0539-8

Tan YL, Yu FH, Ning JG (2015) Design and construction of entry retaining wall along a gob side under hard roof stratum. Int J Rock Mech Min Sci 77:115-121. http://dx.doi.org/10.1016/j.ijrmms.2015.03.025

Tang JX, Hu H, Tu XD et al (2010) Experimental on roadside packing gob-side entry retaining for ordinary concrete. J Chin Coal Soc 35(9):1425-1429. doi:10.13225/j.cnki.jccs.2010.09.015

Wang J, Ning J, Jiang L et al (2018) Structural characteristics of strata overlying of a fully mechanized longwall face: a case study. J S Afri Min Metall 118(11):1195-1204. http://dx.doi.org/10.17159/2411-9717/2018/v118n11a10

Wang Q, Jiang ZH, Jiang B et al (2020) Research on an automatic roadway formation method in deep mining areas by roof cutting with high-strength bolt-grouting. Int J Rock Mech Min Sci 128: 104264. https://doi.org/10.1016/j.ijrmms.2020.104264

Wang BN, Dang FN, Chao Wei et al (2019a) Surrounding rock deformation and stress evolution in pre-driven longwall recovery rooms at the end of mining stage. Int J Coal Sci Technol 6(4): 536-546

Wang J, Ning JG, Qiu PQ et al (2019b) Microseismic monitoring and its precursory parameter of hard roof collapse in longwall faces: a case study. Geomech Eng 17(4):375-383. https://doi.org/10.12989/gae.2019.17.4.375

Wu HK, Liu CW, Zhang Z et al (2020) Time effect of chloride erosion on physical and mechanical properties of high-water-content materials. Adv Mater Sci Eng 1-9. https://doi.org/10.1155/2020/2730283

Xia JW, Su Q, Liu DD (2018) Optimal gypsum-lime content of high water material. Mater Lett 215: 284-287. https://doi.org/10.1016/j.matlet.2017.12.050

Xie ZZ, Zhang N, Feng XW et al (2019) Investigation on the evolution and control of surrounding rock fracture under different supporting conditions in deep roadway during excavation period. Int J Rock Mech Min Sci 123:104122. https://doi.org/10.1016/j.ijrmms.2019.104122

Xie SR, Wang E, Chen DD et al (2020) Failure analysis and control mechanism of gob-side entry retention with a 1.7-m flexible-formwork concrete wall: A case study. Eng Fail Anal 117:104816. https://doi.org/10.1016/j.engfailanal.2020.104816

Yang HY, Cao SG, Wang SQ et al (2016) Adaptation assessment of gob-side entry retaining based on geological factors, Eng. Geol 209:143-151. https://doi.org/10.1016/j.enggeo.2016.05.016

Yu WJ, Liu FF (2018) Stability of close chambers surrounding rock in deep and comprehensive control technology, Adv Civ Eng 1-18. https://doi.org/10.1155/2018/6275941

Yu WJ, Wu GS, An BF et al (2019) Experimental study on the brittle-ductile response of a heterogeneous soft coal rock mass under multi factors coupling. Geofluids 1-15. http://dx.doi.org/10.1155/2019/5316149

Zhang N, Xue F, Zhang NC et al (2015) Patterns and security technologies for co-extraction of coal and gas in deep mines without entry pillars. Int J Coal Sci Technol 2(1):66-75. https://doi.org/10.1007/s40789-015-0058-1

Zhang GC, He FL, Jia HG et al (2017) Analysis of gate road stability in relation to yield pillar size: a case study. Rock Mech Rock Eng 50:1263-1278. https://doi.org/10.1007/s00603-016-1155-1

Zhang FT, Wang XY, Bai JB et al (2020) Post-peak mechanical characteristics of the high-water material for backfilling the gob-side entry retaining: from experiment to field application. Arab J Geosci 13(11):386. https://doi.org/10.1007/s12517-020-05369-9

Zhou XL, Liu CW, Liu YC et al (2020) Effect of dry-wet cycling on the mechanical properties of high-water materials. Adv Civ Eng 1-11. https://doi.org/10.1155/2020/2605751